Storm Surges in the Region of Western Alaska

WARREN BLIER

Department of Atmospheric Sciences, University of California, Los Angeles, Los Angeles, California

STANLEY KEEFE

Weather Forecast Office, National Weather Service—Alaska Region, Anchorage, Alaska

WILSON A. SHAFFER

Office of Systems Development, Techniques Development Laboratory, National Weather Service, Silver Spring, Maryland

SUNG C. KIM

School of Marine Science, Virginia Institute of Marine Science, College of William and Mary, Gloucester Point, Virginia

(Manuscript received 9 September 1996, in final form 10 April 1997)

ABSTRACT

Within the period of the historical record there have been several occurrences of extensive damage from storm-surge-related coastal flooding in the region of Nome, Alaska. The most recent of these events, although by no means the most destructive, occurred in association with the storm of 5–6 October 1992. Despite the small population of Nome (approximately 4000 people), total damage costs exceeded $6 million.

The research into the nature and causes of such flooding events has focused on this October 1992 case. The authors have, however, also examined a weaker, shorter-duration event that occurred on 20 August 1993 and, for contrast, a case in September 1993 where a sustained offshore wind transported water out of Norton Sound. Tide gauge data from Nome were used to quantitatively assess the associated changes in water level, and meteorological analyses were utilized to examine the associated synoptic-scale circulations and their evolution.

In addition, numerical modeling experiments were conducted using an extratropical storm surge model. (A version of this model is operational for the east coast of the United States.) Hindcasts of phase and amplitude for the October 1992 and September 1993 events agreed well with observations. Simulations of the shorter-duration August 1993 event were in poorer agreement with observations and indicate several possibilities for future improvement of the performance of the surge model: enhancement of the horizontal and temporal resolution of the model domain; more accurate input sea level pressure and wind data; and improvements to the surge model itself (e.g., inclusion of sea ice). Overall, however, results indicate that recent operational implementation of the model should be of significant benefit to coastal forecasters.

1. Introduction

The western coast of Alaska has experienced a number of coastal flooding events resulting from storm surges associated with extratropical cyclones. These "storm surges" are abnormally high water levels produced by the meteorological influences of cyclones; the storm surge is defined as the algebraic difference between the measured tide and the predicted astronomical tide. As many of the communities in western Alaska are situated on low-lying coastal land, they are vulnerable to such flooding. This is particularly true for villages built on sandspits, barrier islands, and river deltas.

Two regions along the Bering Sea coast that appear to be especially susceptible to large variations in water level are Norton Sound and Bristol Bay (Fig. 1). Amplification of storm-induced changes in sea level is particularly notable in the former, with its west-facing opening and shallow average depth (approximately 20 m). Repeated destructive flooding events have occurred in the coastal city of Nome (situated on the northwest shore of Norton Sound as indicated in Fig. 1), the largest city in western Alaska, where water levels have risen as much as 4 m.

In the present century there have been at least 14 occurrences of flooding in Nome; all except two occurred in the fall (Wise et al. 1981). That these events generally occur during this time of the year is unsur-

Corresponding author address: Dr. Warren Blier, Department of Atmospheric Sciences, University of California, Los Angeles, 405 Hilgard Avenue, Los Angeles, CA 90095-1565.
E-mail: blier@atmos.ucla.edu

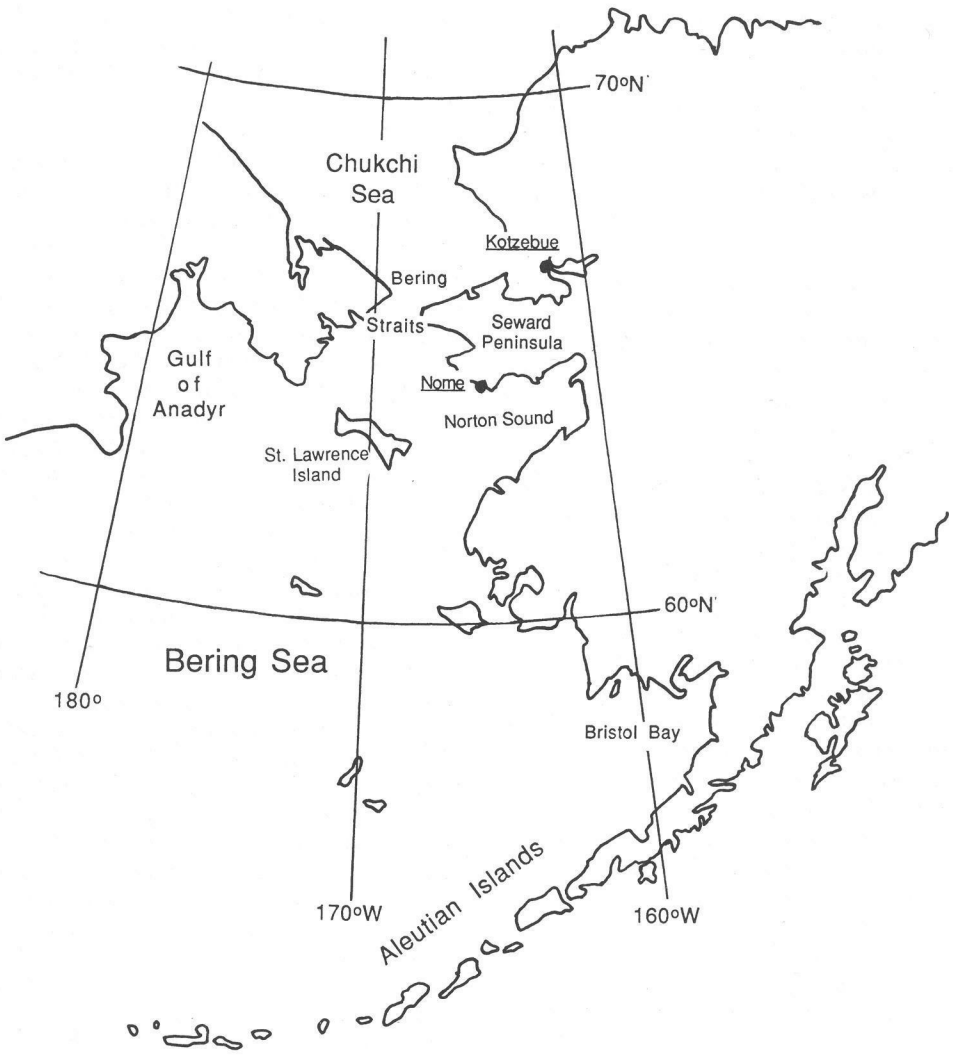

FIG. 1. Map of the region of interest; key locations referred to in the text are indicated.

prising, as Norton Sound is typically ice-covered from mid-to-late November until late in the spring, while the strong surface pressure gradients needed over the Bering Sea for significant coastal flooding to occur are unlikely until at least late summer. During the great storm of early October 1913, for example, ocean waves broke over the top of the city; many of the buildings along Front Street in Nome (situated along the waterfront and the main business street of the town) were torn from their foundations and thrown across the street into other structures. By the end of the storm, the central business district and the east end of the city had been completely destroyed, while a native village (and other houses) on a nearby sandspit had entirely disappeared (Cole 1984).

After a number of destructive storm surges, construction of a sea wall was completed in 1951 to protect the city of Nome. On 11–12 November 1974, Nome was struck by one of the most powerful storms in its history. Despite the presence of the seawall, Nome was severely damaged, with damage to the city estimated at $12–15 million. Significant flooding also occurred along many other stretches of the coast of western Alaska. The meteorological aspects of this surge event are documented by Fathauer (1975); he indicates that at the time of maximum water level in Nome, the actual water level was 4.0 m (13.2 ft) above mean lower low water (MLLW, the long-term average level of the lower low water of the day at a particular location), with 3.8 m (12.5 ft) of this rise attributed to the storm surge [the remaining 0.2 m (0.7 ft) resulted from tidal influences, which are small in this region]. Water that overflowed from the harbor and that went over the sea wall into the city reached a depth of 1.5 m (5 ft) in the lower-lying west end of Nome.

Given the recurrent nature of coastal flooding in western Alaska and the damage it causes, the National Weather Service (NWS) has considered it a priority to provide timely warning of such events. In this regard,

a statistical model was developed to predict storm surges along the coast of Alaska. Various parameters from the comprehensive Alaskan storm surge climatology developed by Wise et al. (1981) were correlated with the surge height through a regression analysis. However, the accuracy, and thus the operational value, of the guidance provided by this model have generally proven to be quite limited.

More accurate forecasting of storm surge events has awaited the development and implementation of a dynamic storm surge forecast model. In the present paper we describe the development and application of such a model to the west coast of Alaska. Evaluation of the quality of the model guidance, as well as more general study of storm surge events in the vicinity of Nome, has been greatly facilitated by the installation of a permanent tide gauge in Nome harbor in June 1992. This represents the only permanent National Oceanic and Atmospheric Administration (NOAA) tide gauge in coastal western Alaska. As a result, a continuous quantitative measurement of water level is now available.

Fortuitously, the most significant coastal flooding episode since the November 1974 event occurred during 5–6 October 1992, soon after the installation of the tide gauge. This was the first (and thus far only) major coastal storm surge event to have occurred since the Nome tide gauge data have become available. An extensive database of meteorological data and analyses was compiled for this case and examined in conjunction with the tide gauge data in order to better understand the nature of these coastal surge events. Given the magnitude of the event and the wealth of data available, this case provided an ideal first test for the newly developed dynamic storm surge model for coastal western Alaska.

To further examine the capabilities of this surge model, two other surge events were also investigated. The first of these occurred in August 1993, and although in certain meteorological respects it at least superficially resembled the October 1992 event, the associated increases in water level were of much smaller magnitude and shorter duration. The other case occurred in September 1993. In this event the low-level winds in the vicinity of Nome were offshore rather than onshore and thus lowered the water level. Such lowering of the water level can have significant adverse impacts on vessels moored in harbor as well as on local fishing boats and maritime shipping traffic, especially given the shallow water depths in the coastal waters of the Bering Sea (including Norton Sound and the waters around Nome). Simulation of such an outflow event also provides a useful test of the more general capabilities of the storm surge model.

2. The extratropical storm surge model

The extratropical storm surge (E-T surge) model is based on the depth-integrated quasi-linear shallow-water equations, as in the dynamic surge forecast model developed by the NWS for tropical cyclones: the Sea, Lake, and Overland Surges from Hurricanes (SLOSH) model (Jelesnianski et al. 1992). However, there are significant differences between surges associated with tropical and extratropical cyclones; thus the tropical model cannot be applied directly to the extratropical situation. In particular, extratropical storm surge models cannot rely on simple parameterized wind fields as are used in the tropical case. Each extratropical cyclone is associated with very different wind (and pressure) characteristics. Rather than obtaining the wind field from a simple parametric model, winds and pressures from one of the operational models of the NWS are used to force the hydrodynamics of the surge model. An additional difference is that time and length scales characterizing extratropical cyclones are typically much greater than those associated with tropical cyclones. The attendant larger grid size and longer time of influence result in increased computational requirements.

A storm surge is primarily the barotropic response of coastal water to the atmospheric forcing, with the dynamics of the surge controlled by variations in the bathymetry of the ocean bottom and the geometry of the coastline. Successful surge forecasting will therefore be critically dependent upon the accuracy of both the bathymetry and the atmospheric forcing. Depth data were constructed from the NOAA ETOPO5 (Earth Topography-5 Minute) global topographic-bathymetric dataset (5-min resolution) and interpolated onto the computational grid; the nearshore bathymetry was extracted manually from nautical charts. For the hindcasts of the three cases examined in the present study, values of the atmospheric forcing terms (mean sea level pressure and lowest sigma-level winds) were obtained from the 12-h analysis fields of the National Meteorological Center (NMC, now known as the National Centers for Environmental Prediction) aviation (AVN) model (Kalnay et al. 1990; Kanamitsu et al. 1991) at a spatial resolution of 2.5° latitude by 2.5° longitude (no higher-resolution historical AVN model output was available to us). Wind values were linearly interpolated in space and time to the model grid. Of course, in operational application, predicted wind values from the appropriate AVN model *forecast* would be used after the initial time.

The domain over which the storm surge model was implemented is shown in Fig. 2a. The elliptical/hyperbolic grid was generated following the grid transformation of Jelesnianski et al. (1992); high-resolution spacing is maintained near the coast (Fig. 2b), while computational economy is achieved through the lower-resolution grid spacing farther offshore.

For further details on the mathematical formulation of the E-T surge model and the numerical schemes utilized, the reader is referred to Jelesnianski et al. (1992) and Kim et al. (1996).

3. The October 1992 storm surge event

The magnitude of the water rise produced by the October 1992 storm surge is indicated by the trace of tide

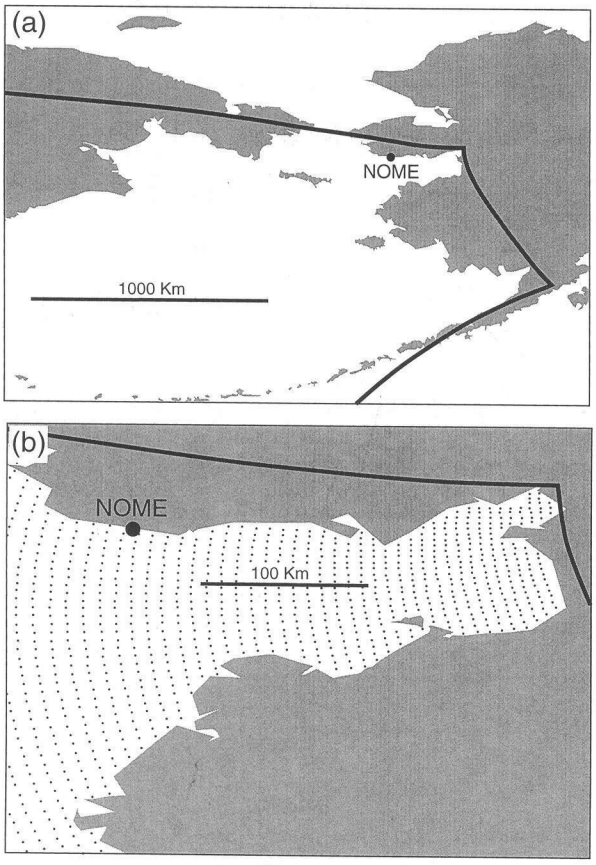

FIG. 2. (a) Domain over which surge model is implemented (grid continues to the west and south). (b) Grid detail in the region of Norton Sound and Nome.

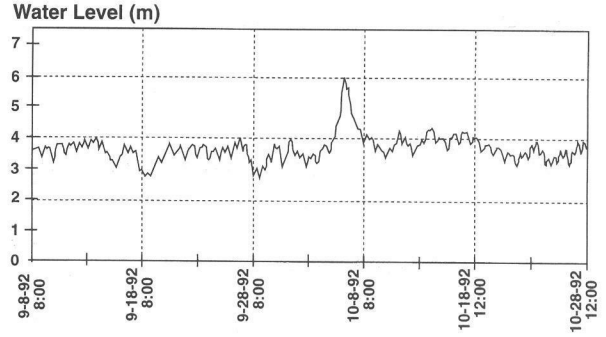

FIG. 3. Trace from Nome tide gauge for the period 8 September to 28 October 1992. Water level (m) above the gauge reference is indicated along the ordinate while date and time (UTC) are indicated on the abscissa.

gauge readings shown in Fig. 3. Immediately evident is the small range of the diurnal tidal fluctuations at Nome, with the difference in water level between low and high tide on the order of 0.5 m. This is much smaller than the approximately 2.5-m increase in water level associated with the early October storm. A magnified view of tide gauge output during the storm appears in Fig. 4. Highest water occurred just prior to 1100 UTC 6 October 1992, culminating a 30-h period of increasing water levels. The height of the seawall at the location of the tide gauge is 8.3 m, while that protecting the business district of the town is 7.9 m high (on the scale of Fig. 4). Thus the peak water level remained 1.8 m below the top of the town seawall. However, the tide gauge data do not include wave height. In the present case, significant flooding in Nome resulted from waves breaking over the sea wall. Superimposed on Fig. 4a are the hourly peak wind gusts from the NWS observing station in Nome. Good correlation is evident between the increase in wind speed and the rise in water level. The hourly surface observations from Nome in Table 1 show that the average surface wind speed was also high, with the wind blowing almost directly onshore. In Fig. 4b, the sea level pressure curve is superimposed on the tide gauge trace. Lowest pressure and strongest wind gusts occurred at approximately the same time as the highest water.

The Nome observations shown in Table 1 further indicate that a frontal passage occurred at approximately 1300 UTC, or about 2 h after the time of high water. Prior to this time, winds at Nome were out of the southeast and south-southeast, with winds shifting to the south-southwest behind the front. Polar-orbiting Defense Meteorological Satellite Program (DMSP) infrared satellite imagery for 0630 UTC 6 October (Fig. 5) indicates that the rear edge of the frontal band was still well to the west of Nome at that time. Similar timing of the high water with respect to the frontal passage was also seen in the November 1974 case (Fathauer 1975).

The 0000 UTC 6 October operational surface analyses from the National Weather Service Forecast Office (WSFO) in Anchorage are shown in Fig. 6. Although the frontal motion and evolution as depicted in these subjective analyses does not appear to be entirely consistent, the basic nature of the overall synoptic development is clearly evident. At 0000 UTC 6 October, a 974-mb low center was analyzed over the eastern Gulf of Anadyr, with its associated occluded front extending to the southeast to a location just west of St. Lawrence Island, and then farther to the south. A developing surface frontal wave is depicted, with the associated low pressure center at 58°N, 175°W. A very strong west–east pressure gradient is evident over the entire portion of the Bering Sea to the east of the front, consistent with reports of strong winds from the south through southeast. Significant deepening occurred during the ensuing 12 h; at 1200 UTC 6 October a single 962-mb low was analyzed over the far eastern tip of Russia, with the occluded front extending to the southeast from the low center and lying along the southwestern coast of the Seward Peninsula just to the west of Nome (Fig. 6b). With the further northeastward movement of the front and surface low, west-southwesterly winds covered most of the Bering Sea, though Norton Sound (and Nome) still experienced the strong south-southeasterly winds ahead of

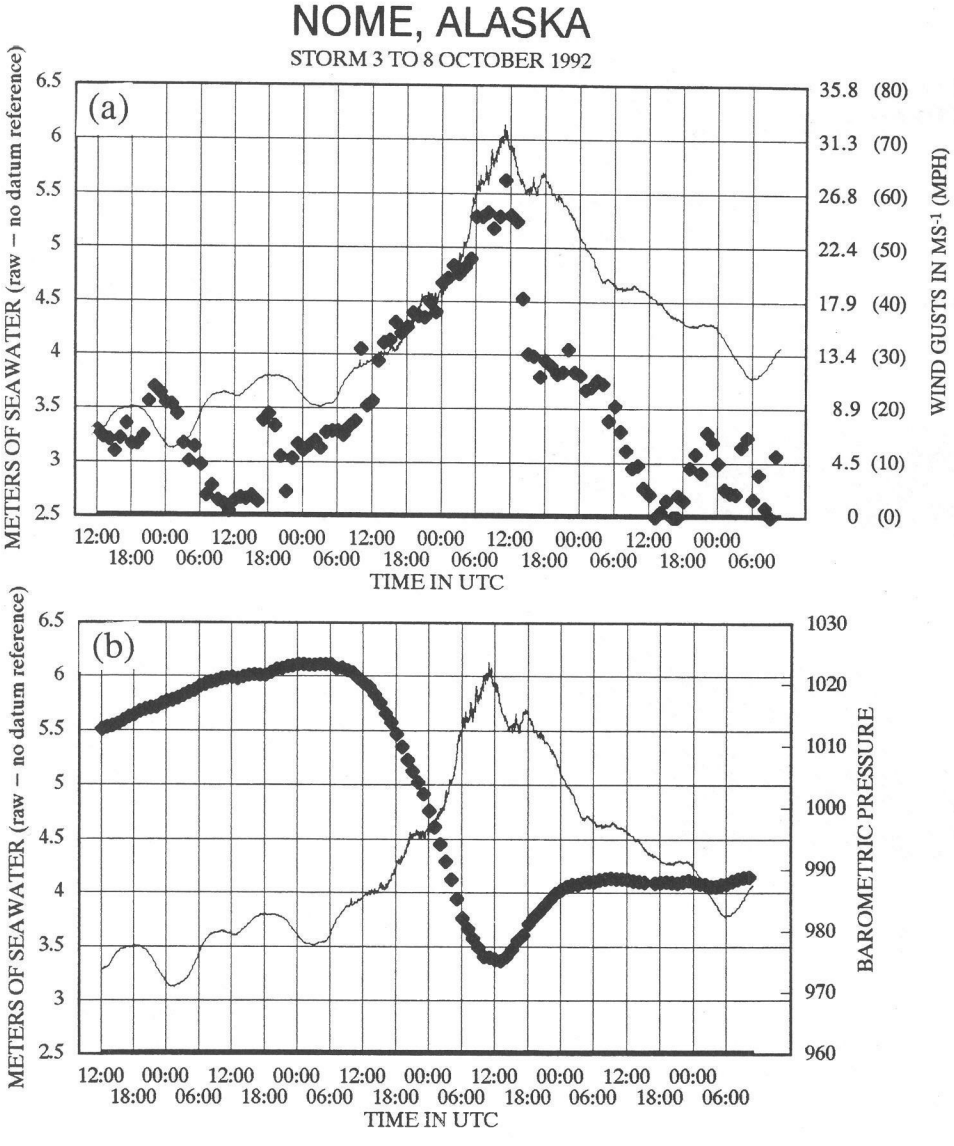

FIG. 4. High-resolution Nome tide gauge data showing variation in water level (solid line, m) for the period 1200 UTC 3 October 1992 to 1200 UTC 8 October 1992 along with (a) peak wind gust (diamonds, m s^{-1}), and (b) sea level pressure (diamonds, mb).

the front. By 0000 UTC 7 October (Fig. 6c), the surface low had moved northward through the Chukchi Sea and begun to weaken, while west-southwest winds prevailed throughout the Bering Sea and Norton Sound.

NMC 500-mb analyses bracketing the time of maximum water level in Nome are shown in Fig. 7. At 0000 UTC 6 October (Fig. 7a), there was strong southwesterly flow aloft into western Alaska, with the 500-mb ridge axis centered over Alaska. Similar to the November 1974 storm surge event, the 500-mb ridge initially developed over the west coast of Alaska (not shown); Fathauer (1975) notes that the presence of a strong ridge aloft in this area is a very reliable precursor of stormy weather along the western Alaska coast. An intense short-wave trough is evident to the south of the Gulf of Anadyr (Fig. 7a) and just to the west of the wave on the surface front noted in Fig. 6a. This upper-level short wave moved rapidly to the northeast during the ensuing 24 h, to a location just southwest of Nome and the Seward Peninsula at 1200 UTC 6 October (not shown), and then moved north of Alaska and over the Arctic Ocean as it weakened (Fig. 7b). Very strong southerly winds aloft preceded this trough as it approached the Seward Peninsula; the plotted 500-mb wind report from the 1200 UTC Kotzebue sounding (not shown, see Fig. 1 for location of Kotzebue) was approximately 40 m s^{-1}. By 0000 UTC 7 October, the upper-level ridge had moved eastward to the region of the Alaska–Yukon Territory border, with westerly and significantly weaker flow over the northern Bering Sea.

TABLE 1. Nome (OME) weather observations from 0252 to 1556 UTC 6 October 1992.

Time (UTC)	T (°C)	T_d (°C)	SLP (mb)	Wind (kt)	Weather	Remarks
0252	−0.6	−1.1	992.3	ESE 30 G39	Light snow, fog	Press falling rapidly
0357	0.0	0.0	988.9	ESE 28 G33	Light snow, fog	Press falling rapidly
0422	—	—	—-	ESE 25 G32	Light snow, fog	
0455	0.6	−0.6	985.9	SE 26 G37	Light snow, fog	Press falling rapidly
0555	1.7	1.7	982.7	SE 36 G46	Light rain, snow, fog	Press falling rapidly
0655	1.1	0.0	980.8	SSE 36 G45	Light rain, snow, fog	
0705	—	—	—-	SSE 34 G45	Light rain, snow, fog	
0754	1.1	0.0	979.3	SE 31 G38	Light rain, snow, fog	
0855	1.1	0.6	977.8	SSE 31 G40	Light rain, snow, fog	
1054	2.2	1.1	975.9	SSE 37 G50	Light rain, snow, fog	
1153	2.2	1.7	975.7	SSE 33 G44	Light rain, fog	
1251	2.8	1.7	975.6	SSE 28 G34	Light rain, fog	
1355	2.8	2.2	976.1	S 23 G30	Light rain, fog	
1450	2.2	1.1	977.2	SSW 17	Light rain, fog	
1537	—	—	—-	SSW 19	Light rain, fog	
1556	2.2	2.2	978.9	SSW 17	Light rain, fog	

The storm surge hindcast for this case was begun at 0000 UTC 3 October 1992 [approximately 83 h prior to the time of high water (1100 UTC 6 October)] and run for 120 h. Lowest sigma-level winds (representative of winds at an elevation of approximately 30 m) and sea level pressure from the 12-h AVN model analyses from 1200 UTC 5 October through 0000 UTC 7 October are shown in Fig. 8. Model output for surge height is shown in Fig. 9 [note that only the first 5 ft (1.5 m) of surge height are explicitly distinguished], while the model output for surface and bottom stress, and mean current for the region of Norton Sound, is shown in Figs. 10–13. As the surface low center approaches from the region of the Kamchatka Peninsula (Fig. 8a), increasing south-southeasterly winds develop over the Bering Sea. In response to these surface winds, water levels along the southwestern shore of the Seward Peninsula and the extreme northwestern part of Norton Sound begin to rise (Fig. 9a). A weak northward vertical mean current transports water into this region (Fig. 10a), as a moderate north-northwestward surface stress develops over the western and northwestern part of Norton Sound in response to the circulation of the approaching cyclone (Fig. 10b). Little bottom stress yet appears (Fig. 10c).

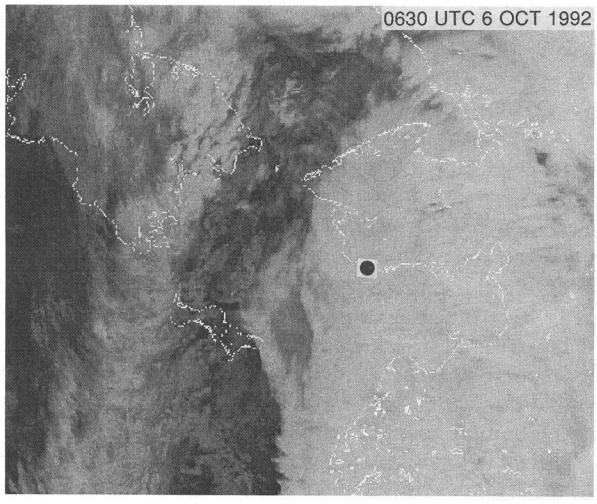

FIG. 5. Polar-orbiting (DMSP) infrared satellite imagery for 0630 UTC 6 October 1992. Heavy dot indicates location of Nome.

By 0000 UTC 6 October (Fig. 8b), a large swath of very strong south-southeasterly winds extends from the Aleutian Islands to the Chukchi Sea north of the Bering Straits. Water levels have now risen significantly in the northwestern part of Norton Sound, with highest water levels along the southwestern coast of the Seward Peninsula (Fig. 9b). In the extreme southeastern part of the Sound, however, water levels are still largely unchanged. A large net mean current into Norton Sound now appears, with a secondary circulation transporting water to the west-northwest along the south shore of the Seward Peninsula (Fig. 11a). Strong surface stresses from the southeast cover the region of Norton Sound as surface winds throughout the area increase from the southeast (Fig. 11b), while significant bottom stress has also now developed (Fig. 11c). Nome tide gauge data (Fig. 4) indicate that the water level has risen significantly by this time.

The highest water level observed in Nome occurred approximately 1 h prior to the time of Fig. 8c (1200 UTC 6 October). At 1200 UTC 6 October, west-southwesterly surface flow covers most of the Bering Sea, as the northwest–southeast-oriented surface frontal trough is situated just to the southwest of Nome. Surface winds by the entrance to Norton Sound are now out of the southwest, while southeasterly flow remains over the eastern end of the Sound. The simulated region of maximum surge height has now enlarged and expanded eastward into Norton Sound (Fig. 9c), with maximum water heights extending westward along its north shore from the general vicinity of Nome to the western tip of the Seward Peninsula. Substantial net transport of water into Norton Sound is evident (Fig. 12a), except for the nearshore countercurrent in the extreme northwestern part

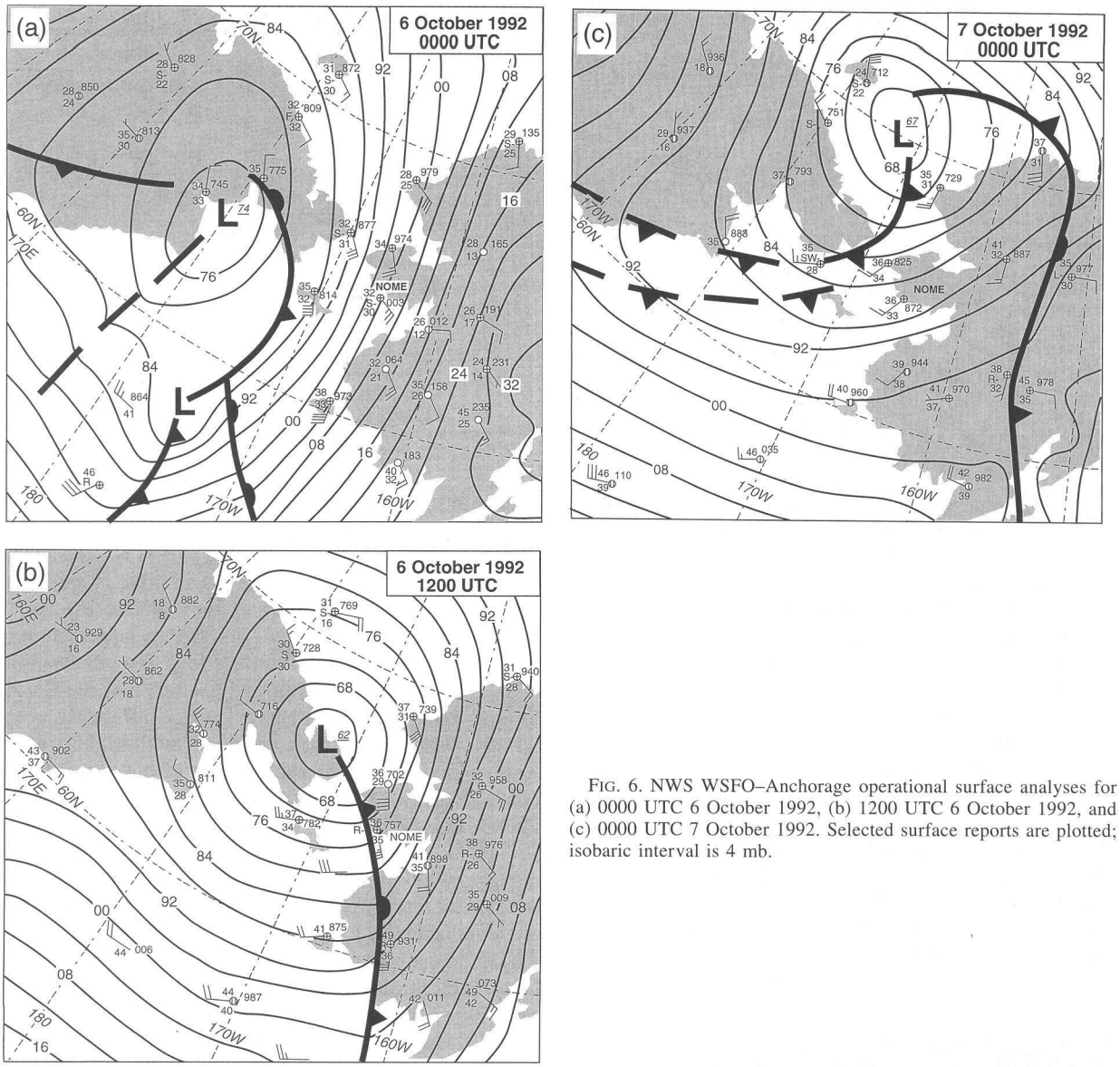

FIG. 6. NWS WSFO–Anchorage operational surface analyses for (a) 0000 UTC 6 October 1992, (b) 1200 UTC 6 October 1992, and (c) 0000 UTC 7 October 1992. Selected surface reports are plotted; isobaric interval is 4 mb.

of the sound. The depicted mean current results in substantial local transport of water into the southern coast of the central Seward Peninsula and toward the far eastern part of the Sound. The proximity of the occluded front is indicated by the variation in the orientation of the surface stress vectors—from southwesterly by the entrance to Norton Sound to southeasterly by its far eastern shore (Fig. 12b). With the increase in magnitude of the mean current and the shallow depth of the waters, the bottom stress also increases significantly (Fig. 12c).

The surge model indicates a continuation of this eastward migration of maximum water levels within the Sound during the subsequent 12 h in conjunction with the eastward propagation of the region of southwesterly surface flow. By 0000 UTC 7 October (Fig. 8d), southwesterly flow behind the front extends over the entire Sound, with the model indicating receding water levels in the vicinity of Nome (Fig. 9d), and even more so in the open waters of the entrance to the Sound, while waters levels have now increased to approximately their maximum height in the far eastern part of the Sound. The mean current has weakened substantially (Fig. 13a), reflecting the large bottom stress evident 12 h earlier (Fig. 12c) the greater similarity in orientation of the surface (Fig. 13b) and bottom stress vectors following the frontal passage, and the reduction in wind speed behind the front. As the mean current weakens, so does the magnitude of the bottom stress (Fig. 13c).

The model-simulated time evolution of water level at Nome is shown in Fig. 14, along with the same Nome tide gauge trace shown in Fig. 4. In comparing the model simulation with the tide gauge measurements, it is im-

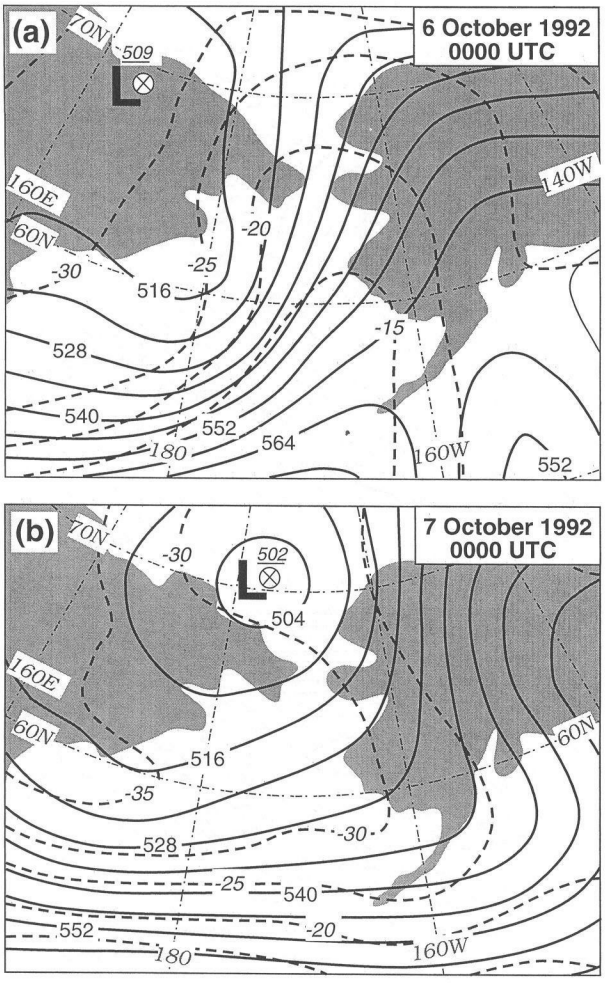

FIG. 7. NMC final 500-mb analyses for (a) 0000 UTC 6 October 1992 and (b) 0000 UTC 7 October 1992. Solid lines are height contours (interval is 6 dam) and dashed lines are isotherms (interval is 5°C).

portant to note that the surge model does not include the astronomical tide. Proper comparison of the model output with the tide gauge measurements thus requires superposition of astronomical tide levels. In Fig. 14, the corresponding adjusted model-predicted water level (i.e., with the astronomical tide also taken into account) is indicated just at 1200 UTC 6 October, the approximate time of highest water level (which happened to occur at about the time of high tide). The surge model thus does an impressive job of capturing the storm surge that occurred in Nome. The timing of the increase (and subsequent decrease) in water level is almost perfectly replicated; the model fails to capture only the last 0.8 m of water rise at the peak of the event. This error is likely a consequence of several factors: the low spatial and temporal resolution of the wind and pressure data input from the AVN model analyses (2.5° latitude by 2.5° longitude, and 12 h, respectively); and errors present in the AVN model analyses, not at all unlikely given the data-sparse nature of the region. Although the AVN sea level pressure fields in Figs. 8b,c in general compare reasonably well with the corresponding NWS WSFO–Anchorage subjectively analyzed sea level pressure fields in Figs. 6a,b, some significant differences do appear. Most important among these, perhaps, is the absence of any indication in the 0000 UTC 6 October AVN sea level pressure field of the frontal wave and associated low pressure center depicted on the subjective analysis for the same time. Given these limitations and sources of error, the performance of the surge model appears to be quite impressive, at least at the site of the Nome tide gauge.

The absence of other tide gauges in the region and of other quantitative water level data makes it difficult to verify the the timing and magnitude of the hindcast at locations other than Nome. To assess the magnitude of the storm surge produced by the earlier November 1974 storm in the region, Sallenger (1983) quantitatively examined the debris line elevation at various locations along the northern and eastern shores of Norton Sound. As he noted, debris line elevations provide a combined measure of (a) sea level rise due to wind setup (the rise in nearshore water level caused by wind-induced net shoreward transport of water, which is enhanced in shallow bodies of water such as Norton Sound), (b) inverse barometric effect (water level rises as sea level atmospheric pressure decreases, though less than 0.5 m for a 50-mb pressure decrease), (c) wave setup (local increase in mean sea level in surf zone), and (d) wave run-up (shore elevation reached by wave upwash). Although not explicitly mentioned by Sallenger, a fifth factor affecting water level and debris line elevation is the astronomical tide—though as noted earlier, tidal influences in the region of Norton Sound are small. Debris lines tend to be found somewhat lower than the height of maximum run-up, but higher than the maximum still-water level during the storm. Thus debris line elevation gives a measure of the rise in water level due to the storm surge itself plus the additional effects of the astronomical tide (small) and wave run-up. (The latter, of course, does not appear in tide gauge measurements). Sallenger found that at all but a few locations, the 1974 storm had incorporated older debris lines and pushed them higher—thus, he generally observed only one debris line.

Although lacking the time and resources to perform a similarly detailed survey of the Norton Sound driftwood line for the October 1992 storm, in September 1995 the authors did undertake a more qualitative and cursory examination of the relative heights above water level (under quiescent conditions) of the driftwood line at various locations along the length of the south shore of the Seward Peninsula and the northern half of the far eastern shore of Norton Sound. As the region is very sparsely populated, driftwood in most locations tends to remain where deposited by significant storms.

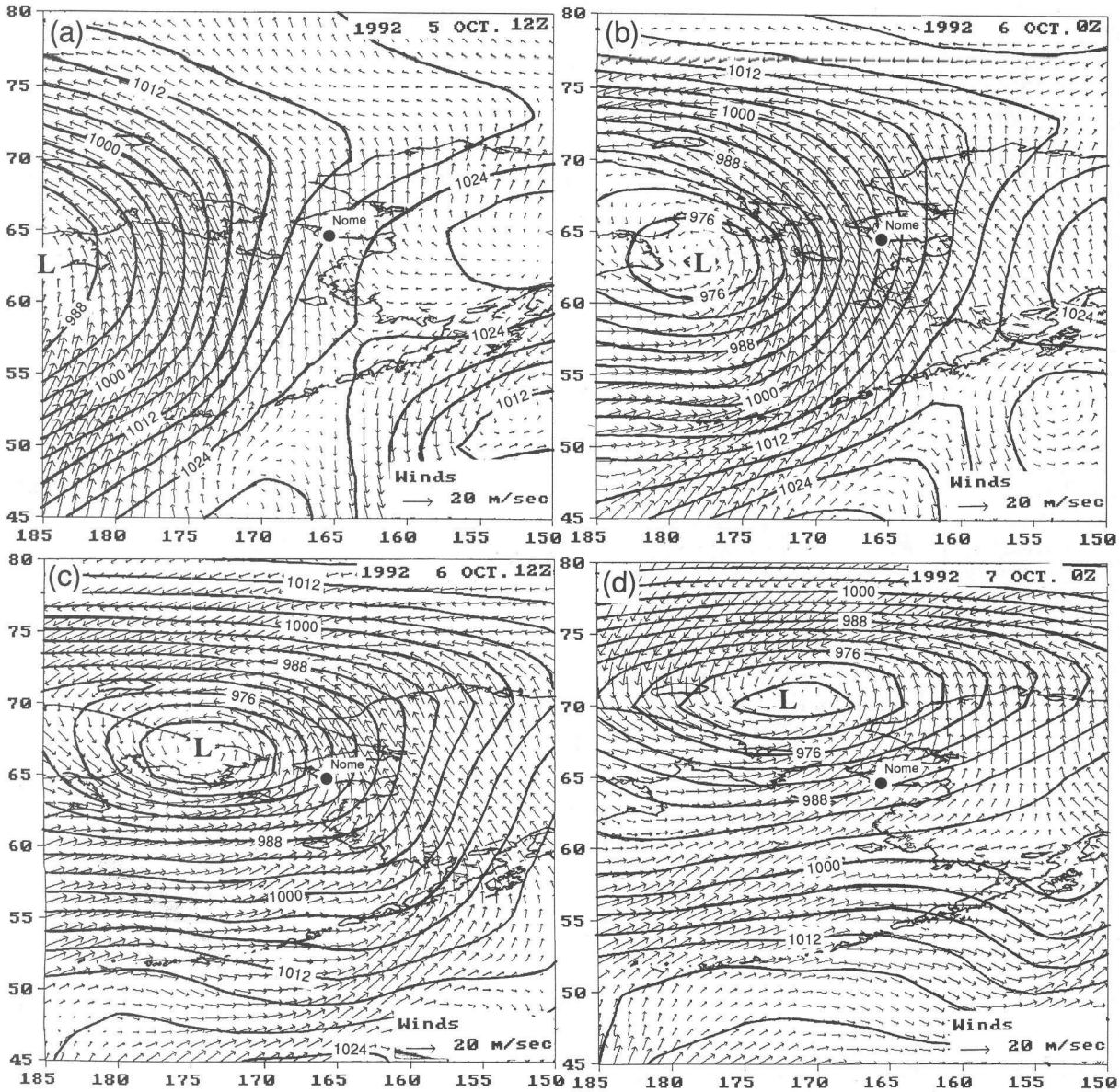

FIG. 8. AVN model analyses of sea level pressure and lowest sigma-level wind for (a) 1200 UTC 5 October, (b) 0000 UTC 6 October, (c) 1200 UTC 6 October, and (d) 0000 UTC 7 October 1992. Isobaric interval is 4 mb; scaling for surface wind vectors is indicated in the inset.

In most locations, two driftwood lines were evident at significant elevations above the water surface—one from the November 1974 storm and the other from the October 1992 storm. Qualitative assessment indicated highest elevation of the driftwood line from the October 1992 storm along the north coast of the Sound in the region approximately 60—100 km east of Nome. At a few locations within this region, only a single driftwood line was found, indicating that a higher total water level (as described above) was reached than in even the November 1974 storm (for which Sallenger showed storm surge heights of 4.0 m in the same area). This is consistent with the model output [not shown—surge heights greater than 5 ft (1.5 m) not explicitly indicated in Fig. 9].

Although not examined by either Sallenger or in the present study, it should be noted that even though substantial driftwood was found along the entire length of the north shore of Norton Sound, no trees are found in the western part of the Seward Peninsula, which is covered with tundra. Thus it is conceivable that assessment of circulations and transport within the waters of Norton Sound, at least in major storms, could be facilitated by further examination of driftwood lines.

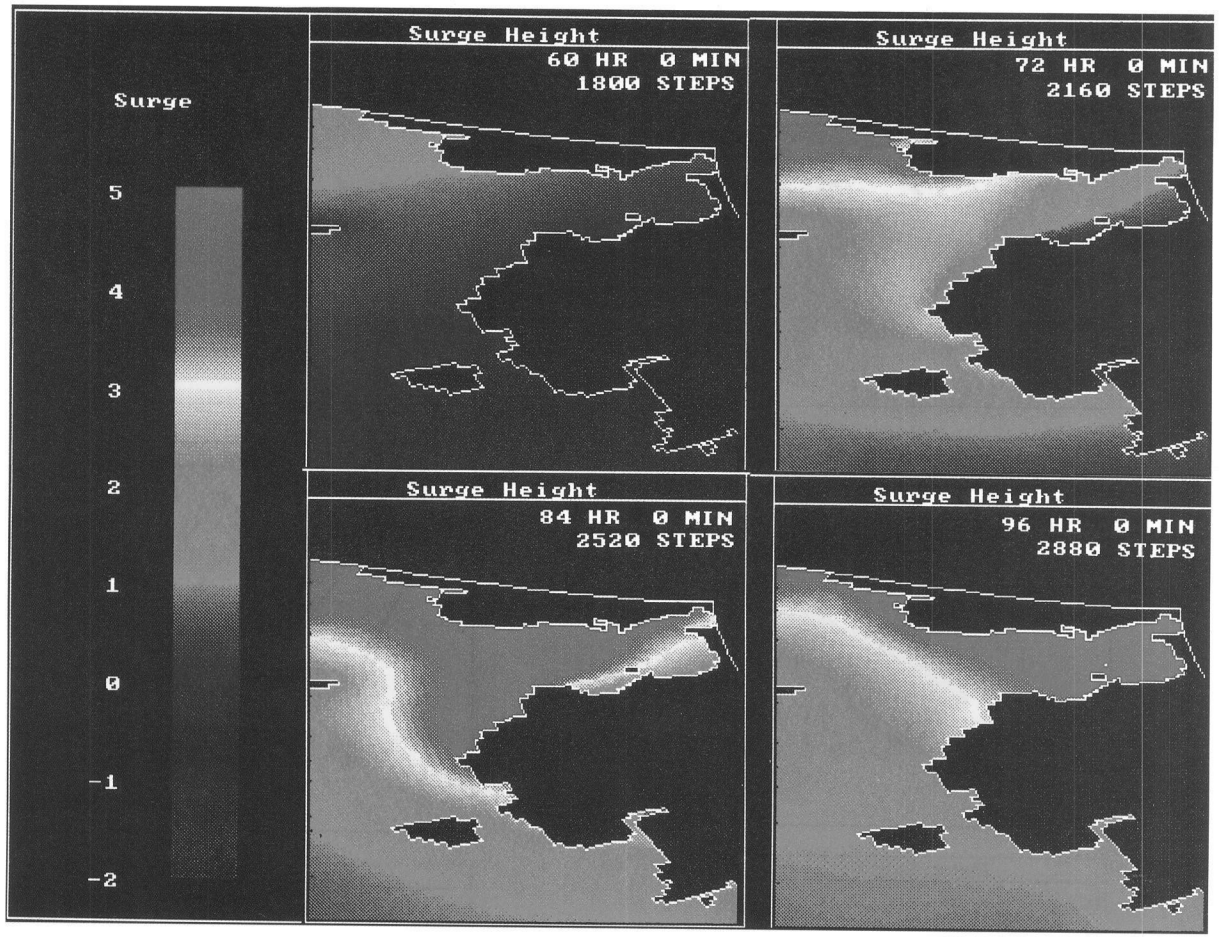

FIG. 9. Hindcast surge model output for surge height (ft) at (a) hour 60 (1200 UTC 5 October 1992), (b) hour 72 (0000 UTC 6 October) (c) hour 84 (1200 UTC 6 October 1992), and (d) hour 96 (0000 UTC 7 October 1992). (Note that 5 ft = 1.52 m.)

4. The August 1993 storm surge event

A trace of Nome tide gauge output for a 3-month period beginning 1 July 1993 is shown in Fig. 15. Several significant departures from the usual diurnal tidal variation are apparent. The present discussion will focus on the elevated water level event of 20 August 1993, while the subsequent section will consider the reduction in water level that occurred on 20–21 September 1993.

On 20 August 1993, a storm surge resulted in a brief elevation of the water level in Nome of 1.2 m (peak water level occurred at 1500 UTC 20 August). Comparison of this event with the much more significant and longer-duration storm surge of October 1992 reveals that magnitude of the surge is very dependent on the track followed by the surface cyclone. In the October 1992 case, the surface cyclone and associated front approached the Bering Straits from the west-southwest; ahead of it a wide swath of strong south-southeasterly surface flow covered the entire meridional extent of the Bering Sea (Fig. 8). In the August 1993 event, however, the surface cyclone approached the Bering Straits from the south-southeast (Fig. 16). At 0000 UTC 19 August, the surface low was centered over the western portion of Bristol Bay (not shown). During the ensuing 12 h, the low moved to the northwest, to a position approximately 200 km to the southeast of St. Lawrence Island at 1200 UTC 19 August (Fig. 16a). As Norton Sound was then in the northeast quadrant of the low, surface winds over the Sound were out of the east-southeast. Continued movement of the low to the northwest resulted in a wind flow more conducive to increased water levels in Nome (and along the north shore of Norton Sound) by 0000 UTC 20 August (Fig. 16b). This favorable wind flow was short lived, however, as the low weakened significantly during the next 12 h (8-mb increase in central pressure), as did the pressure gradient around it. At 1200 UTC 20 August (not shown), predominantly westerly flow covered most of the Bering Sea south of St. Lawrence Island, while winds over Norton Sound backed to southeasterly ahead of a surface trough approaching from the south. These AVN surface analyses compare favorably with the corresponding

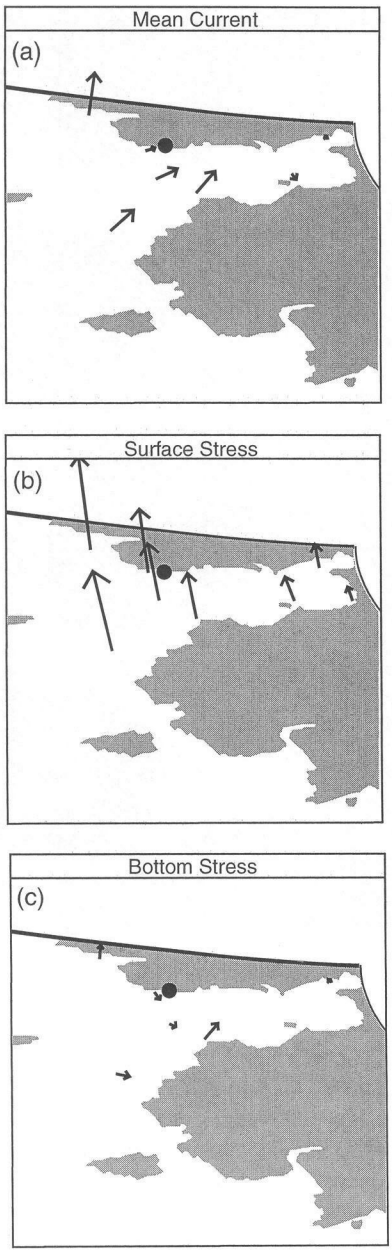

FIG. 10. Hindcast surge model output at hour 60 (1200 UTC 5 October 1992) for (a) selected mean current vectors, (b) selected surface stress vectors, and (c) selected bottom stress vectors. Relative magnitude proportional to length of vector. Heavy dot indicates location of Nome.

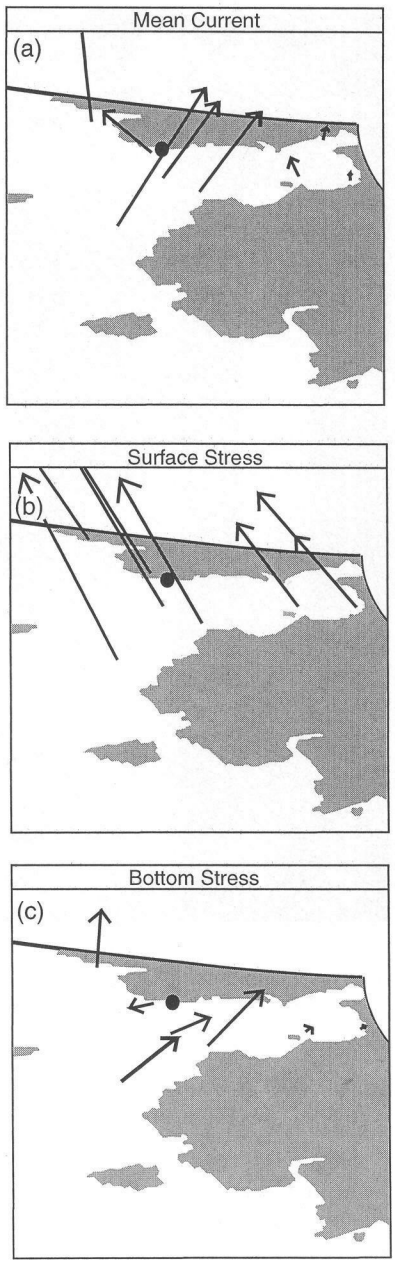

FIG. 11. Same as Fig. 10 except at hour 72 (0000 UTC 6 October 1992).

WSFO–Anchorage subjective surface analyses (not shown).

Comparison of Fig. 16b (15 h prior to highest water in Nome in the August 1993 event) with Fig. 8b (11 h prior to highest water in Nome in the October 1992 event) shows not dissimilar locations and central pressures of the two surface lows. Pressures were much higher over the interior of Alaska in the October case, however, resulting in a comparatively stronger pressure gradient over a wider region to the east of the low. (That sea level pressures were significantly higher over the interior of Alaska in an October event than in an August event is unsurprising given the climatological cooling that occurs between these months.) In addition, the shape of the low in the October case and the somewhat more easterly position of its center were both more conducive to south-southeasterly flow over a much larger region of the central and eastern Bering Sea. The difference in paths, however, appears to have been the most significant influence on the difference in the magnitudes

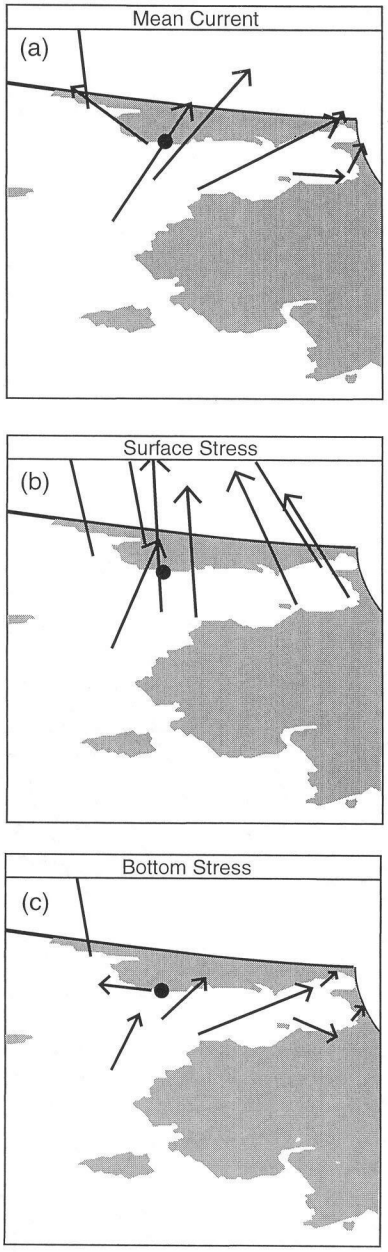

FIG. 12. Same as Fig. 10 except at hour 84 (1200 UTC 6 October 1992).

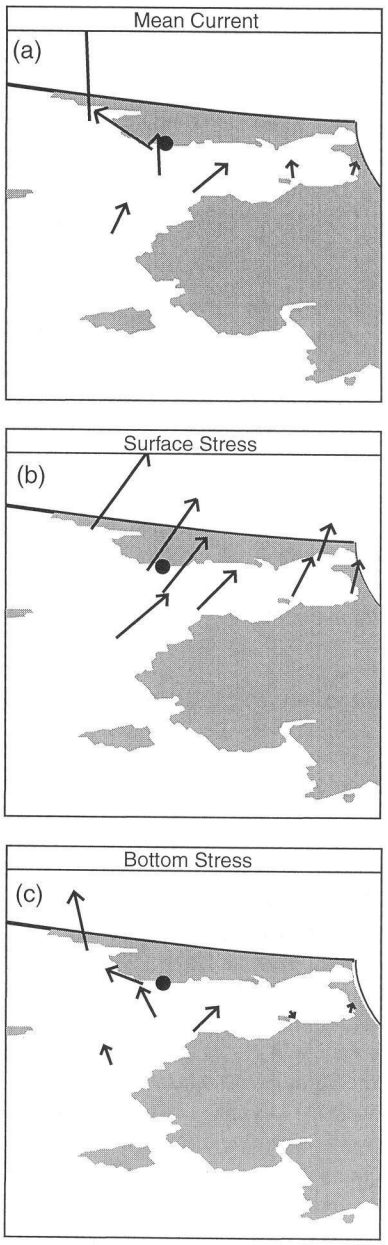

FIG. 13. Same as Fig. 10 except at hour 96 (0000 UTC 7 October 1992).

of the storm surges experienced in Nome. In the August 1993 case, favorable winds for elevated water levels in Norton Sound were comparatively short lived and only occurred over the far eastern part of the Bering Sea. The large fetch of south-southeasterly flow that developed over much of the central and eastern Bering Sea in the October 1992 case never occurred in the August 1993 case. (Interestingly, in the August case, the surge model did predict a much more significant rise in water level along the northeastern shore of Bristol Bay, which appeared to experience a more favorable wind flow for a longer duration of time. Unfortunately, no observational data were available to verify the surge model prediction in that area.)

The E-T surge model did not accurately simulate the 20 August 1993 surge event in Nome. Figure 17 shows a comparison of the surge model output with the tide gauge data. The relatively brief duration of the event appears to have been the most significant factor limiting the accuracy of the model output—given the 12-h interval between times of input of surface pressures and winds from the AVN model analyses (and thus 12-h-long periods through which these fields must be deter-

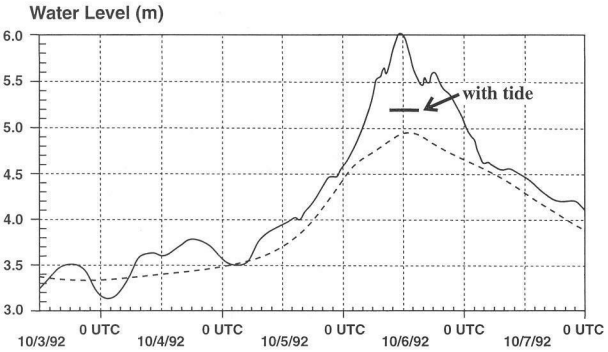

FIG. 14. Hindcast surge model water level heights (dashed line) and Nome tide gauge measurements (solid line). Model initialized at 0000 UTC 3 October 1992. See text for further details.

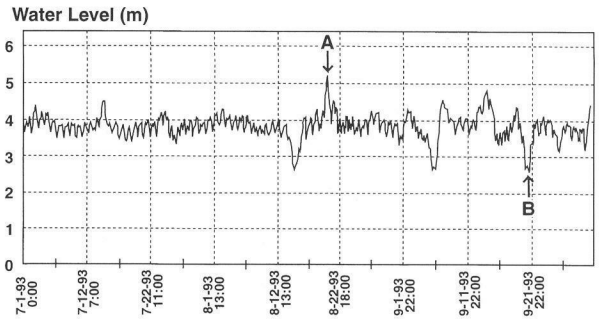

FIG. 15. Trace from Nome tide gauge for the period 1 July through 1 October 1993. Arrows A and B indicate the 20 August 1993 and 20–21 September 1993 events, respectively. Other conventions as in Fig. 3.

mined from linear interpolation in time). The operationally implemented version of the model uses a 3-h interval and thus may better capture these shorter-duration, weaker events.

5. The September 1993 storm surge event

On 20–21 September 1993, strong north-northeasterly flow developed over the Seward Peninsula and Norton Sound. As a result, water was transported out of Norton Sound, as evidenced by the corresponding reduction in water level indicated in Fig. 15. This offshore flow developed in response to a deepening surface low that moved northeastward from latitude 175°W over the Aleutian Island chain at 1200 UTC 19 September (Fig. 18a) to just south of the eastern end of Norton Sound at 0000 UTC 21 September (Fig. 18b). After this time, the low weakened as it continued to move to the northeast over the interior of Alaska.

Throughout this event, surface winds at Nome were out of the north-northwest and thus approximately 180° out of phase with those in the October 1992 positive surge event. Also, as the timescale for this case was more comparable to the longer timescale of the October 1992 surge (Figs. 3 and 4) than the very short timescale of the August 1992 surge (Figs. 15 and 17), we felt it would provide a good test of the robustness of the surge model, namely, its ability to also simulate wind-driven *outflow* of water from Norton Sound. In fact, the model hindcast for this event was remarkably good. Comparison of the model prediction with the tide gauge values (Fig. 19) shows excellent agreement in both phase (timing) and amplitude. As noted previously, astronomical tides are not included in the model; low tide occurred at about 0000 UTC 21 September, which is approximately the time of the first of the two minima in water level that occurred during this event (the other occurred 12 h later). The variation between this low tide and the preceding high tide, however, was less than 0.5 m.

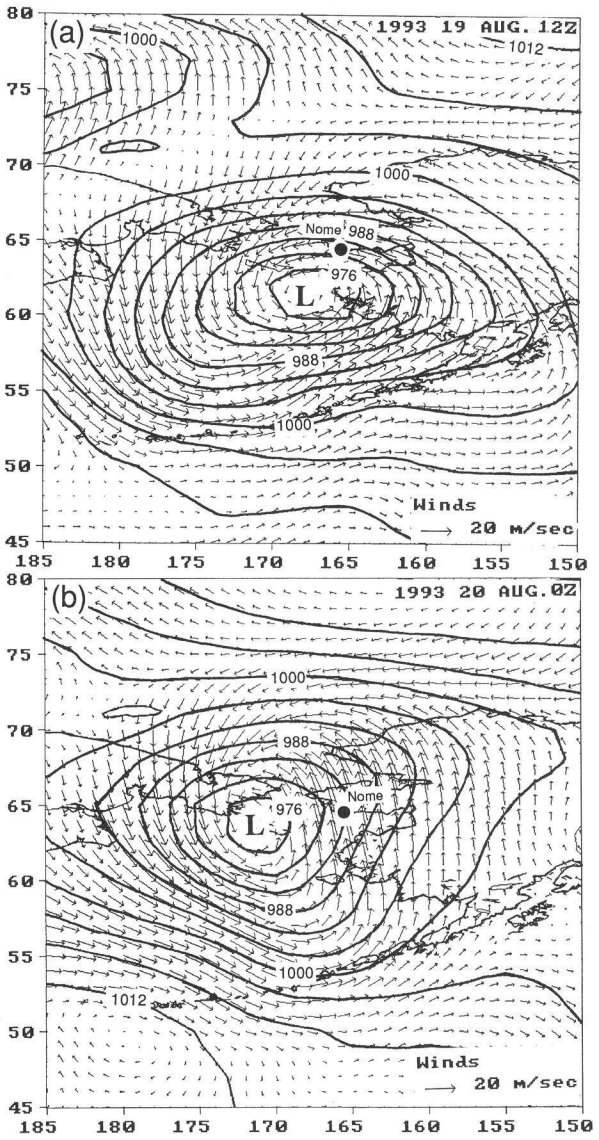

FIG. 16. Same as Fig. 8 except for (a) 1200 UTC 19 August and (b) 0000 UTC 20 August 1993.

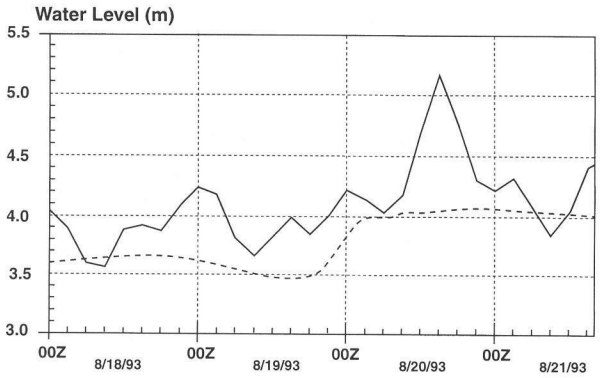

FIG. 17. Hindcast surge model water level heights (dashed line) and Nome tide gauge measurements (solid line). Model initialized at 0000 UTC 17 August 1993.

6. Summary and concluding remarks

Three storm-surge events in the region of Nome, Alaska, have been examined meteorologically and simulated with the E-T surge model. The October 1992 high surge event was associated with a large and persistent area of strong south-southeasterly surface flow that developed to the east of a deep surface low moving northeastward over the western portion of the Bering Sea. The surface development was associated with a shortwave trough embedded in strong southwesterly flow at 500 mb ahead of an amplifying upper-level ridge. The surge model performed well at Nome, though it failed to capture the entire increase in water level. The hindcast for the September 1993 negative surge event, which occurred as a surface cyclone centered to the southeast of Nome produced strong north-northwesterly flow, was also very impressive. The significantly shorter-duration August 1993 surge event, however, was not well simulated. The low spatial and temporal resolution of the wind data input from the AVN model likely limited the ability of the model to accurately replicate the observed brief increase in water level. Previous applications of the surge model to the United States east coast indicate that use of similarly low-resolution data resulted in degraded predictions for short-duration events associated with fast-moving systems.

In this regard, the recently implemented operational version of this surge model in Alaska utilizes 1° latitude by 1° longitude wind and sea level pressure values from the AVN model output at 3-h intervals (rather than the 2.5° by 2.5° data output at 12-h intervals as in the present study). It is expected that the higher-resolution input from the AVN model will lead to better predictions by the surge model. One possible mitigating factor must also be considered, however. As the operational surge model generates forecasts, it will require input of forecast surface wind and pressure fields from the AVN model; for the hindcasts presented here, AVN model analyses could be used instead—and verified by comparison with detailed surface observations and analyses.

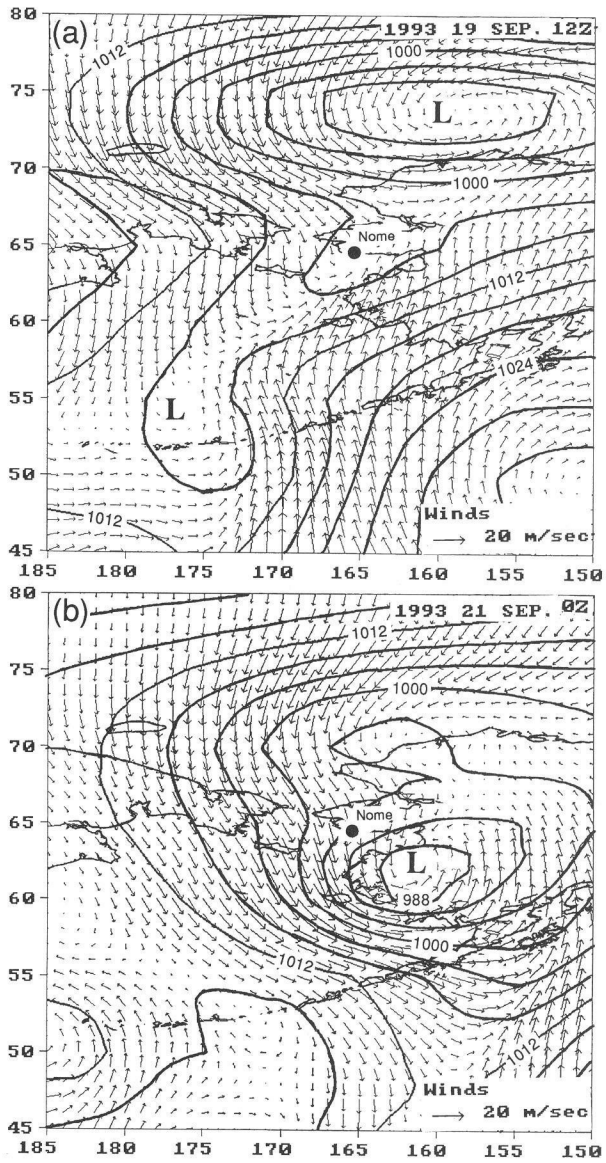

FIG. 18. Same as Fig. 8 except for (a) 1200 UTC 19 September 1993 and (b) 0000 UTC 21 September 1993.

Thus the accuracy of the operational surge model forecasts will depend on the quality of the input forecast information from the AVN model. This surge model has generally worked well on the United States east coast, however, and thus we are optimistic that it will provide valuable guidance to the operational forecaster in Alaska in issuing timely and accurate storm surge warnings. In the future, input of higher-resolution and more accurate forecast surface winds and pressures from, for example, the Pennsylvania State University–National Center for Atmospheric Research (NCAR) Mesoscale Model Version 5 (MM5) (Grell et al. 1995), may lead to further improvements in the surge model forecasts.

In addition, further consideration is needed of the

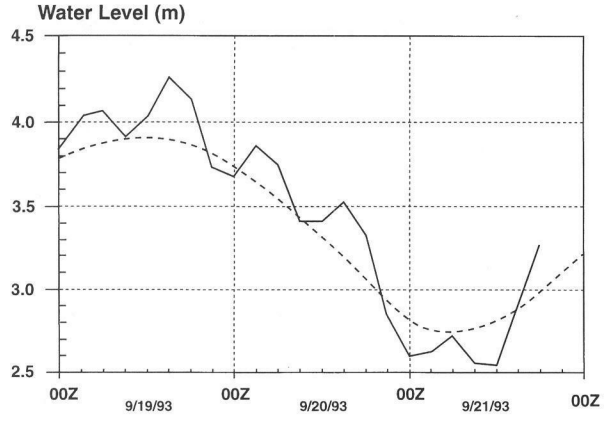

FIG. 19. Hindcast surge model water level heights (dashed line) and Nome tide gauge measurements (solid line). Model initialized at 0000 UTC 17 September 1993.

potential influence of sea ice. For all of the cases considered in the present study, the Bering Sea and Norton Sound were ice-free. However, some of the most significant storm surge events have occurred with sea ice present (e.g., the storm surge events of November 1974 and November 1978). The possible consequences of the presence of sea ice are potentially significant and complex. In the November 1978 case, for example, the shore-fast ice extending several hundred meters offshore from the beach before the storm began was broken up during the event; Fischer (1978) speculates, however, that the broken ice dampened the wave action and therefore resulted in less water coming over the seawall. In contrast, in the November 1974 storm, floating blocks of sea ice aggravated the flood damage to communities in eastern Norton Sound (Fathauer 1978). Johnson and Kowalik (1986) have investigated the influence of the inclusion of shore-fast ice on storm surge modeling in Norton Sound and have found that it can produce measurable differences in the results.

Finally, improved verification of the surge model forecasts in western Alaska will necessitate the availability of tide gauge data from locations other than Nome.

Acknowledgments. This research was supported in part by COMET Grant UCAR S9357 and NOAA's Coastal Oceans Program. Many individuals contributed to the success of this project; we gratefully acknowledge assistance provided by Fabrice Cuq, James Murakami, and John Oleska at UCLA; Brian Bezenek, Dennis Dickson, Jerry Steiger, John Stepentin, and Robert Tschantz at the NWS WSO in Nome; Ted Fathauer and Kraig Gilkey at the NWS WSFO in Fairbanks; Ray Moore and Per Pedersen with PRC Corporation in Anchorage; The Alaska Air National Guard; and Nancy McGuire, publisher of the *Nome Nugget.*

REFERENCES

Cole, T., Ed., 1984: Nome: City of the golden beaches. *Alaska Geogr.* **7,** 1–183.

Fathauer, T. F., 1975: The great Bering Sea storms of 9–12 November 1974. *Weatherwise,* **28,** 76–83.

——, 1978: A forecast procedure for coastal floods in Alaska. NOAA Tech. Memo. NWS AR-23, National Oceanic and Atmospheric Administration, U.S. Department of Commerce, 27 pp. [Available from National Technical Information Service, 5285 Port Royal Road, Springfield, VA 22161.]

Fischer, R. E., 1978: Major Bering Sea storm of November 7–10, 1978 and associated coastal flooding at Nome, Alaska. Forecast Office Final Rep., U.S. National Weather Service, Fairbanks, AK, 15 pp. [Available from National Weather Service Forecast Office, 101 12th Avenue, Fairbanks, AK 99701.]

Grell, G. A., J. Dudhia, and D. R. Stauffer, 1995: A description of the fifth-generation Penn State/NCAR Mesoscale Model (MM5). NCAR Tech Note NCAR/TN-398+STR, 122 pp. [Available from National Center for Atmospheric Research, P.O. Box 3000, Boulder, CO 80307.]

Jelesnianski, C. P., J. Chen, and W. A. Shaffer, 1992: SLOSH: Sea, lake, and overland surges from hurricanes. NOAA Tech. Rep. NWS 48, National Oceanic and Atmospheric Administration, U.S. Department of Commerce, 71 pp. [Available from National Technical Information Service, 5285 Port Royal Road, Springfield, VA 22161.]

Johnson, W. R., and Z. Kowalik, 1986: Modeling of storm surges in the Bering Sea and Norton Sound. *J. Geophys. Res.,* **91,** 5119–5128.

Kalnay, E., M. Kanamitsu, and W. E. Baker, 1990: Global numerical weather prediction at the National Meteorological Center. *Bull. Amer. Meteor. Soc.,* **71,** 1410–1428.

Kanamitsu, M., and Coauthors, 1991: Recent changes implemented into the global forecast system at NMC. *Wea. Forecasting,* **6,** 425–435.

Kim, S. C., J. Chen, and W. A. Shaffer, 1996: An operational forecast model for extratropical storm surges along the U.S. east coast. Preprints, *Conf. on Oceanic and Atmospheric Prediction,* Atlanta, GA, Amer. Meteor. Soc., 281–286.

Sallenger, A. H., 1983: Measurements of debris-line elevation and beach profiles following a major storm: Northern Bering Sea coast of Alaska. U.S. Geological Survey Open-File Rep. 83-394, 10 pp. [Available from USGS Information Services, Box 25286, Denver Federal Center, Denver, CO 80225.]

Wise, J. L., A. L. Comiskey, and D. Becker Jr., 1981: *Storm Surge Climatology and Forecasting.* Arctic Environmental Information and Data Center, 32 pp.